Optimal Spatial Distribution of Microstructure in Porous Electrodes for Li-ion Batteries

Ravi N. Methekar, Vijayasekaran Boovaragavan, Mounika Arabandi, Venkatasailanathan

Ramadesigan, Venkat R. Subramanian, Folarin Latinwo, and Richard D. Braatz, *IEEE Fellow*

Abstract—**This paper applies simultaneous optimization to the design of spatially-varying porosity profiles in next-generation electrodes to maximize the capacity of Li-ion batteries, based on porous electrode theory. This paper designs a porous positive electrode made of lithium cobalt oxide, which is commonly used in lithium-ion batteries for various applications. For a fixed amount of active material, optimal grading of the porosity across the electrode decreases the Ohmic resistance by 25%, which in turn increases the electrode capacity to hold and deliver energy. Over 40% enhancement was observed in the robustness of the optimal electrode designs to variations in model parameters due to manufacturing imprecision. The results are sufficiently promising to justify investment in the development of experimental procedures to fabricate batteries that have a graded porosity across the electrode.**

I. INTRODUCTION

Electrochemical power sources have had significant improvements in design and operating range and are expected to play a vital role in the future in automobiles, power storage, military, and space applications. Lithium-ion chemistry has been identified as a preferred candidate for high-power/high-energy secondary batteries. Applications for batteries range from implantable cardiovascular defibrillators (ICDs) operating at 10 µA current to hybrid vehicles requiring pulses of up to 100 A. Today, the design of these systems have been primarily based on (1) matching the capacity of anode and cathode materials, (2) trial-and-error investigation of thickness, porosity, active material, and additive loading, (3) manufacturing convenience and cost, (4) ideal expected thermal behavior at the system level to handle high currents, and (5) detailed microscopic models to understand, optimize, and design these systems by changing one or few parameters at a time.

Traditionally, macroscopic models have been used to optimize the electrode thickness or spatially uniform porosity in lithium-ion battery design.[1] Many applications of mathematical modeling to design Li-ion batteries are available in the literature.[1-9] An approach to identify the optimal values of system parameters such as electrode thickness has been reported by Newman and coworkers.[5-9] Simplified models based on porous-electrode theory can provide analytical expressions to describe the discharge of rechargeable lithium-ion batteries in terms of the relevant system parameters. Newman and his coworkers[5-8] have utilized continuum electrochemical engineering models for design and optimization as a tool for the identification of system limitations from the experimental data. Equations were developed that describe the time dependence of potential as a function of electrode porosity and thickness, the electrolyte and solid-phase conductivities, specific ampere-hour capacity, separator conductivity and thickness, and current density. Analysis of these equations yield the values of electrode porosity and electrode thickness so as to maximize the capacity for discharge to a given cutoff potential.[5] Simplified models based on porous-electrode theory were used to describe the discharge of rechargeable lithium batteries and derive analytic expressions for the cell potential, specific energy, and average power in terms of the relevant system parameters. The resulting theoretical expressions were then used for design and optimization purposes and also as a tool for the identification of system limitations from experimental data.[6] Studies were performed by comparing the Ragone plots for a range of design parameters. A single curve in a Ragone plot involves hundreds of simulations wherein the applied current is varied over a wide range of magnitude. Ragone plots for different configurations are obtained by changing the design parameters (e.g., thickness) one at a time, and by keeping the other parameters at constant values. This process of generating a Ragone plot is quite tedious, and typically Ragone curves reported in the literature are not smooth due to computational constraints. Batteries are typically designed only to optimize the performance at the very first cycle of operation of the battery, whereas in practice most of the battery's operation occurs under significantly degraded conditions. Further, multivariable optimization is not computationally efficient using most first-principles models described in the literature. A reformulated model[11-12] is

V. Boovaragavan is with Lawrence Berkeley National Laboratory, Berkeley, CA 94720 USA (e-mail: VBoovaragavan@lbl.gov)

M. Arabandi is with the Department of Chemical Engineering, Tennessee Tech University, Cookeville, TN 38505 USA (e-mail: marabandi21@tntech.edu).

R. N. Methekar and V. Ramadesigan are with the Department of Energy, Environmental and Chemical Engineering, Washington University in St. Louis, St. Louis, MO 63130 USA (e-mails: methekarr@seas.wustl.edu and vramadesigan@wustl.edu).

V. R. Subramanian is with the Department of Energy, Environmental and Chemical Engineering, Washington University in St. Louis, One Brookings Drive, Campus Box 1180, St. Louis, MO 63130 USA (phone: 314-935-5676; fax: 314-935-7211; email: vsubramanian@wustl.edu).

F. Latinwo and R.D. Braatz are with the University of Illinois, Urbana, IL 61801 USA (e-mails: latinwo1@illinois.edu and braatz@illinois.edu).

sufficiently computationally efficient to enable the simultaneous optimal design of multiple parameters over any number of cycles by including the mechanisms for capacity fade. Further, this model can be used to quantify the effects of model uncertainties and variations in the design parameters on the battery performance. Recently, such an application was reported in which the utilization averaged over 1000 cycles was maximized for a battery design obtained by simultaneous optimization of the applied current density (I) and thickness of the separator and the two electrodes (l_s, l_n, l_p) for cycle 1, and the effects of variations in these four design parameters due to imprecise manufacturing was investigated.[13] The battery design optimized for cycle 1 did not maximize the cycle-averaged utilization.

This paper applies simultaneous optimization to the design of spatially varying porosity profiles in next-generation electrodes to maximize the capacity of Li-ion batteries, based on porous electrode theory. The optimization procedure is followed by the electrochemical model, the results and discussion, and conclusions.

II. ELECTROCHEMICAL POROUS ELECTRODE MODEL

This paper considers the optimization of a single porous positive electrode, where the electrode has the current collector at one end ($x = 0$) and electrolyte separator at the other end ($x = l_p$). The expressions for current in the solid phase (i_1) and electrolyte phase (i_2) are given by[1]

$$i_1 = -\sigma(x)\frac{d\Phi_1}{dx}; \qquad i_2 = -\kappa(x)\frac{d\Phi_2}{dx} \qquad (1), (2)$$

where σ is the electrical conductivity, κ is the ionic conductivity, and Φ_1 and Φ_2 are the solid-phase and electrolyte-phase potentials, respectively. The total applied current density across the cross-section of the electrode is equal to the sum of the solid-phase and liquid-phase current densities:

$$i_{app} = i_1 + i_2 . \qquad (3)$$

The electrochemical reaction occurs at the solid-liquid interface and relates the solid-phase current (i_1) to the distance across the electrode (x) by the linear kinetics:

$$di_1/dx = a(x)i_0(\Phi_1 - \Phi_2)F/(RT) \qquad (4)$$

where the active surface area is given by

$$a(x) = 3\left(1 - \varepsilon(x)\right)/R_p \qquad (5)$$

R_p is the particle radius of active materials in the porous electrode, and $\varepsilon(x)$ is the spatially-varying porosity in the electrode. The electrical and ionic conductivities are related to the spatially-varying porosity by

$$\sigma(x) = \sigma_0\left(1 - \varepsilon(x)\right); \qquad \kappa(x) = \kappa_0\varepsilon(x)^{brugg} \qquad (6), (7)$$

The boundary conditions for solution of these equations are given as

$$\left.\Phi_1\right|_{x=0} = 1; \quad \left.\Phi_2\right|_{x=l_p} = 0; \quad \left.i_1\right|_{x=l_p} = 0; \qquad (8)$$

where *brugg* is the Bruggman coefficient to account for the tortuous path in the porous electrode. The ohmic resistance of this electrode is obtained by

$$\psi = \frac{\left.\Phi_1\right|_{x=0} - \left.\Phi_2\right|_{x=l_p}}{i_{app}}; \quad i_{app} = -\sigma(x)\frac{d\Phi_1}{dx}\bigg|_{x=0} \qquad (9), (10)$$

The above equations are valid for any continuous or discontinuous functional form for $\varepsilon(x)$ and can be readily extended to more detailed micro-scale models for the conductivities and transport parameters as a function of porosity. Electrochemical engineering models accounting for the effects of local stress, phase transfer in the electrodes, electrodes with two different particle sizes, and thermal behavior have extended the applicability and flexibility. Garcia et al.[14] used a detailed microstructure model to model and identify porosity or particle size variations in the electrodes to maximize performance. Atomistic simulations have predicted new materials with higher energy density, but the physical limit has never been reached in a full-cell design. Previous efforts have been made on atomistic simulations of batteries,[15] microstructural simulations,[16] and modeling the relationships between the properties and microstructure of the materials within packed multiphase electrodes. The effect of this equation on the optimal design of the porous electrode is also considered by analyzing a range of values for Bruggman coefficient.

The electrochemical modeling equations are usually solved by setting the applied current and computing the voltage, or vice versa. However, many practical devices operate at constant current or constant power mode. It is important to realize that the capacity of each device is limited by the state variables and theoretical capacity of the material. To solve the mathematical model for a practical electrochemical device, it is necessary to obtain the physically realizable current value to be applied to or drawn from the electrode.

A. Constant-Current Method

In solving this model for constant-current, the constant current i_{app} is set and the modeling equations are simulated with corresponding boundary conditions for the variables like Φ_1, Φ_2, and i_1 as given below. Then the resistance (ψ) is computed using the output equation.

Modeling equations:

$$i_1 = -\sigma(x)\frac{d\Phi_1}{dx}; \qquad i_2 = -\kappa(x)\frac{d\Phi_2}{dx}$$

$$\frac{di_1}{dx} = a(x)i_0\frac{F}{RT}(\Phi_1 - \Phi_2); \qquad i_{app} = i_1 + i_2$$

$$a(x) = \frac{3\left(1 - \varepsilon(x)\right)}{R_p}$$

Boundary conditions:

$$\left.\Phi_1\right|_{x=0} = 1; \quad \left.\Phi_2\right|_{x=l_p} = 0; \quad \left.i_1\right|_{x=l_p} = 0$$

Output equation:

$$\psi = \frac{\left.\Phi_1\right|_{x=0} - \left.\Phi_2\right|_{x=l_p}}{i_{app}}$$

This procedure is easy to implement and the modeling equations are straightforward to simulate. However, the applied fixed current may not be commensurate with the capacity of the given battery and there is a chance of obtaining physically inconsistent results such as a predicted potential of −100 or +1000 V. To avoid this potential error, the constant-potential method has been used as described in next subsection.

B. Constant-Potential Method

To avoid the shortcoming of the constant-current method, the constant-potential method is used. In this method, the potential (Φ_1, Φ_2) is set and the current is treated as the output. This is done by solving i_{app} as the unknown variable in the model equations. Then the resistance (ψ) is estimated using the output equation.

Modeling equations:

$$i_1 = -\sigma(x)\frac{d\Phi_1}{dx}; \quad i_2 = -\kappa(x)\frac{d\Phi_2}{dx}$$

$$\frac{di_1}{dx} = a(x)i_0\frac{F}{RT}(\Phi_1 - \Phi_2); \quad i_{app} = i_1 + i_2$$

$$a(x) = \frac{3(1-\varepsilon(x))}{R_p}$$

Boundary conditions:

$$\Phi_1\big|_{x=0} = 1; \quad \Phi_2\big|_{x=l_p} = 0; \quad i_1\big|_{x=l_p} = 0$$

$$i_{app} = -\sigma(x)\frac{d\Phi_1}{dx}\bigg|_{x=0}$$

Output equation:

$$\psi = \frac{\Phi_1\big|_{x=0} - \Phi_2\big|_{x=l_p}}{i_{app}} \tag{11}$$

One additional boundary condition has been incorporated for describing the relationship of the applied current with the state variables. The advantage of this procedure is that, the current has been determined using the state variables of the battery instead of being fixed to a preset number by the modeler. This computationally robust approach ensures that the voltage and current are at physically consistent values.

III. Optimization Procedure

A general formulation for the model-based optimal design of a system is[17]

$$\min_{\mathbf{z}(x),\mathbf{u}(x),\mathbf{p}} \Psi \tag{12}$$

$$\text{s.t.} \ \frac{d}{dx}\mathbf{z} = \mathbf{f}(\mathbf{z}(x),\mathbf{y}(x),\mathbf{u}(x),\mathbf{p}), \ \mathbf{f}(\mathbf{z}(0)) = 0, \ \mathbf{g}(\mathbf{z}(1)) = 0, \tag{13}$$

$$\mathbf{g}(\mathbf{z}(x),\mathbf{y}(x),\mathbf{u}(x),\mathbf{p}) = 0, \tag{14}$$

$$\mathbf{u}_L \le \mathbf{u}(x) \le \mathbf{u}_U, \quad \mathbf{y}_L \le \mathbf{y}(x) \le \mathbf{y}_U, \quad \mathbf{z}_L \le \mathbf{z}(x) \le \mathbf{z}_U, \tag{15}$$

where Ψ is the battery design objective to be minimized,[18] $\mathbf{z}(x)$ is the vector of differential state variables, $\mathbf{y}(x)$ is the vector of algebraic variables, $\mathbf{u}(x)$ is the vector of control variables, and $\mathbf{p}$ is the vector of design parameters. Different methods are available for solving constrained optimization problems, which include (i) variational calculus, (ii) Pontryagin's maximum principle, (iii) control vector iteration, (iv) control vector parameterization, and (v) simultaneous nonlinear programming.[17] Control vector parameterization (CVP) is one of the commonly used methods and is the easiest method to implement. In the context of this particular application, the control variable $\mathbf{u}(x)$ is parameterized by a finite number of parameters, typically as a polynomial or piecewise-linear function or by partitioning its values over space, and the resulting nonlinear program is solved numerically. Most numerical optimization algorithms utilize an analytically or numerically determined gradient of the optimization objective and constraints to march towards improved values for the optimization variables in the search space. While advances in simultaneous discretization have been made in the field of dynamic and global optimization,[19] these algorithms are still too computationally expensive to be used for most applications such as electrochemical processes, which are usually highly stiff with highly nonlinear kinetics and requires adaptive time-stepping, stiff solvers, etc. It is not expected that the simultaneous simulation-optimization approach,[17] which fixes the time or independent variable discretization *a priori*, will be computationally efficient for lithium-ion battery applications. In this paper, CVP is used to simultaneously optimize multiple parameters describing a spatial profile of porosity of an electrode in a lithium-ion battery. The numerical optimization was carried out using Marquardt's method,[20] in which new parameter values for the next iteration are related to the gradient multiplied by the old values of the design parameters. The numerical algorithm was repeated until a pre-specified tolerance on the change in the design parameters was met.

In this formulation, the control variable (i.e., porosity) is partitioned across the electrode length. In each partition, the modeling equations described by Eqs. (1) to (11) are solved as a function of porosity. The boundary conditions at each partition are matched using the flux balance of the species. The number of equations is directly proportional to the number of partitions. The number of boundary conditions will also increase with the number of equations and partitions. The optimization objective was to minimize the Ohmic resistance (ψ) across the electrode thickness in Eq. (1) for the control variable $u(x) = \varepsilon(x)$ subject to the constraints

a) $0 < \varepsilon(x) < 1$

b) Average $\{\varepsilon_i\} < 0.4$, where $i = 1,\dots,N$ (when a specific amount of active material is desired)

c) Eqs. (1) to (11), where $\mathbf{y}(i) = [\Phi_{(1,i)}, \Phi_{(2,i)}, i_{(1,i)}]$ and $0 \le x \le l_p$

$$i_{(1,i)} = -\sigma_i(x)\frac{\partial\Phi_{(1,i)}}{\partial x}; \quad i_{(2,i)} = -\kappa_i(x)\frac{\partial\Phi_{(2,i)}}{\partial x}$$

$$\frac{\partial i_{(1,i)}}{\partial x} = a_i i_0 \frac{F}{RT}(\Phi_{(1,i)} - \Phi_{(2,i)})$$

$$a_i = \frac{3\left(1 - \varepsilon_i(x)\right)}{R_p}$$

d) Boundary conditions for accommodating the partitions across the electrode are

$$\Phi_{(1,i)}\Big|_{x=l_p/N} = \Phi_{(1,i+1)}\Big|_{x=0}$$

$$\Phi_{(2,i)}\Big|_{x=l_p/N} = \Phi_{(2,i+1)}\Big|_{x=0}$$

$$i_{(1,i)}\Big|_{x=l_p/N} = i_{(1,i+1)}\Big|_{x=0}$$

where i indicates the ith partition and $x = 0$ and $x = l_p/N$ indicate the starting and ending spatial boundaries of the ith partition. The non-negativity constraint is imposed on the porosity and the average-value constraint is imposed when specific amount of active material is desired in the electrode. The Ohmic resistance is calculated as a function of the porosity from the modeling equations. The model equations along with fixed boundary conditions and boundary conditions arising from CVP were solved using a Boundary Value Problem (BVP) solver. Table 1 shows the basic set of parameters used for the simulation of the model equations (1)-(11) at various conditions. All simulations are performed using Maple® 13's BVP solver using a personal computer with a 3 GHz processor and 3.25 GB of RAM. The equations were reformulated to reduce computational cost, as described in prior publications.[12-13]

IV. RESULTS AND DISCUSSIONS

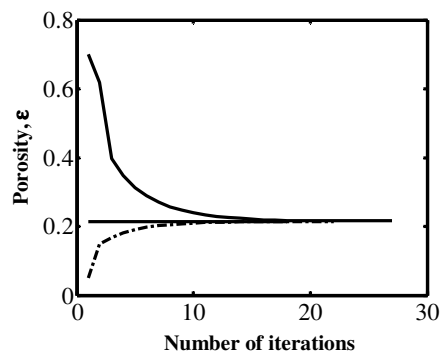### A. Optimization Results For Uniform Porosity

Fig. 1 shows the variation in the ionic resistance of the organic electrolyte solution across the electrode as a function of spatially-uniform porosity obtained by brute-force gridding of the porosity, which shows a clearly identifiable optimal porosity of about 0.2. Operating with the porous electrode at this optimum porosity should provide the best performance for a system described by the model (1)-(11).
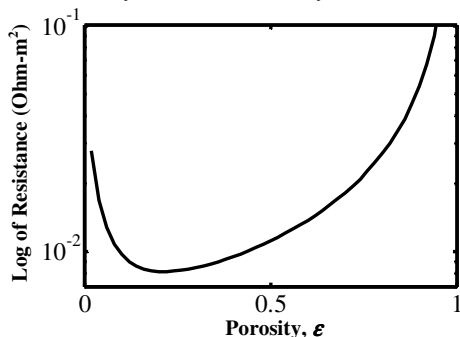
Fig. 1 Resistance versus porosity, ε. The plot was constructed by computing the resistance from the model equations (5)-(11) for each spatially-uniform porosity between 0 and 1.

Fig. 2a shows the convergence of the numerical optimization to the globally optimal value of the spatially-uniform electrode porosity. This plot was constructed by optimizing the electrochemical model described in Section 2 starting at three different initial guesses (third guess being the optimal value obtained in Fig. 1) for the electrode

porosity. The final converged value for the electrode porosity was the same for many different initial guesses (two of which are shown in Fig. 2a). Fig. 2b shows the convergence of the Ohmic resistance across the electrode to the same single optimal value. A very low resistance was achieved by using the globally optimal value for the porosity of the electrode. Significant improvements in terms of performance were achieved by numerical optimization; the optimal design is about 15% more efficient in comparison with an average value of 0.4 used in practice for the electrode porosity for this chemistry.

Fig. 2(a) Convergence to the optimal spatially-uniform porosity ε starting from different initial guesses for the porosity
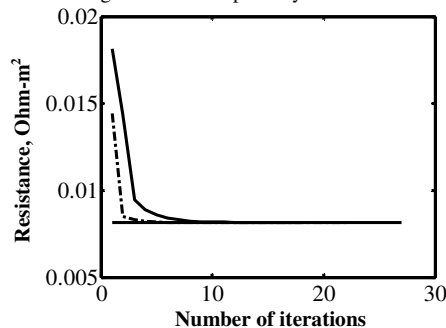
Fig. 2(b) Corresponding convergence of the Ohmic resistance.

B. Optimization Results For Graded Porosity

Numerical optimization was performed for a porous electrode with a graded porosity, that is, porosity that varies as a function of distance across the electrode. The porosity profile was divided into N optimization zones, with constant porosity within each zone (see Fig. 3). For $N = 5$, the resistance across the electrode is minimized when the porosity is higher towards the electrode-separator interface (see Fig. 4), to have more electrolyte solution in the porous matrix. The optimal profile shows a significant decrease in pore volume at the other end, at the electrode-current collector interface. This optimization procedure shows improvement of electrode performance of 17.2% compared to the base-case spatially uniform porosity of 0.4. The spatially optimized electrode porosity has 4% better performance than the optimal spatially-uniform porosity for the same chemistry. Batteries with more complicated chemistry models or different chemistry models, and optimization with additional physical constraints on the design, can have different performance improvements when using spatially-varying porosity. Increasing the value of the number of zones N above 5, while being more difficult to

fabricate, does not show much improvement in the performance. For instance, an improvement of 0.1% was obtained for $N = 12$ compared to $N = 5$. The choice of $N = 5$ provides a good tradeoff between optimality and manufacturability.

Now consider the same optimal design problem but with the additional constraint of having a specified amount of active material in the electrode, which is equivalent to having a fixed value for the porosity averaged across the electrode. For a fixed average porosity $\varepsilon_0 = 0.3$, the performance improvement is 15% compared to the base case, while having an optimal porosity profile that is qualitatively similar to that without the average porosity constraint (compare Figs. 4a and 5a). A qualitatively similar optimal porosity profile is obtained for a fixed average porosity $\varepsilon_0 = 0.5$, while providing a performance improvement of 33% over the base case. The performance improvement of 33% compared to 20% for Fig. 4 is due to the increased number of optimization zones.
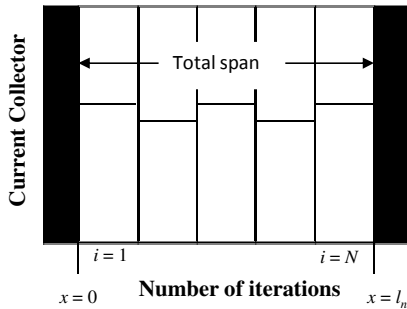

Fig. 3 Schematic of an electrode of a lithium-ion battery divided into N optimization zones.

Fig. 6 shows the applied current profile across the electrode for optimized and base-case design. The optimized current at the electrode-current collector interface is higher in magnitude due to lower resistance. The spatial variation in the electrolyte-phase potentials follow a similar qualitative trend but are very different quantitatively (see Fig. 7). The solid-phase potential in both cases does not show much variation across the electrode (see Fig. 8). The net potential drop $(\Phi_1 - \Phi_2)$ at the electrode-current collector interface is greater in the base case compared to the optimized case, indicative of the much lower resistance inside the cell with optimized porosity profile.
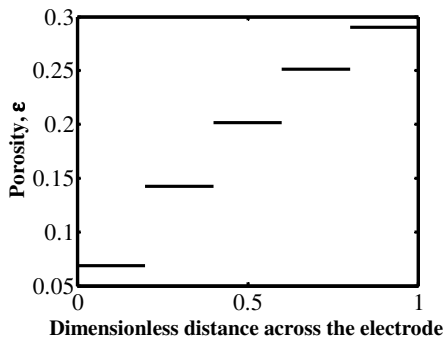

Fig. 4 Optimal porosity profile for $N = 5$ optimization zones.

Due to limited manufacturing precision and capacity fade, model parameters will vary somewhat from one electrode to the next. The importance of quantifying the effects of such uncertainties on the performance of microstructured materials is well established.[21] The probability distribution functions (pdfs) for the Ohmic resistance for spatially-uniform electrode porosities indicate that the optimized design is more robust to uncertainties in comparison to a non-optimized porosity, with a reduction in variance for the optimal design of about 36% (see Fig. 9). The design with the optimized spatially-varying porosity is slightly more robust, with a reduction of variation of about 42% compared to a non-optimized porosity (see Fig. 10). The robustness could be further enhanced by explicitly including uncertainty quantification into the optimization formulation.

V. CONCLUSION

Model-based optimization was applied to the design of spatially varying porosity profiles in next-generation electrodes to minimize the Ohmic resistance in Li-ion batteries, based on porous electrode theory. The implementation of control vector parameterization is demonstrated for a porous electrode model for the cobalt oxide chemistry in commercial lithium-ion batteries. The optimal design of graded porosity was found to reduce Ohmic resistance by at least 25% without increasing the amount of active material. Over 40% enhancement in the performance robustness of the optimal electrode designs was observed. The results are sufficiently promising to justify investment in the development of experimental procedures to fabricate batteries that have a graded porosity across the electrode. It is expected that further investigations into a whole-cell battery model will lead to a significant engineering design alternatives that can meet energy and power requirements for emerging applications for batteries in vehicles, satellites, and in the military.
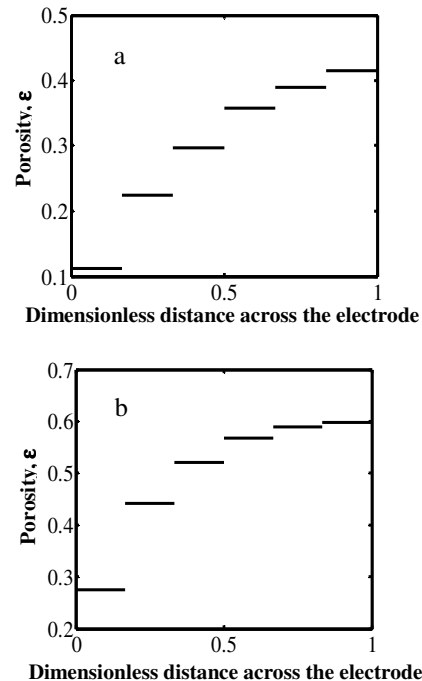

Fig. 5 Optimum porosity profile for $N = 6$ optimization zones for a fixed average porosity of (a) 0.3 and (b) 0.5.

REFERENCES

[1] M. Doyle, T. F. Fuller, J. Newman, *J. Electrochem. Soc.*, **140**, 1526 (1993).
[2] T. Fuller, M. Doyle, J. Newman, *J. Electrochem. Soc.*, **141**, 1 (1994).
[3] T. F. Fuller, M. Doyle, J. Newman, *J. Electrochem. Soc.*, **141**, 982 (1994).
[4] J. Newman, *J. Electrochem. Soc.*, **142**, 97 (1995).
[5] W. Tiedemann, J. Newman, *J. Electrochem. Soc.*, **122**, 1482 (1975).
[6] M. Doyle, J. Newman, *J. Power Sources*, **54**, 46 (1995).
[7] M. Doyle, J. Newman, *Electrochim. Acta*, **40**, 2191 (1995).
[8] V. Srinivasan, J. Newman, *J. Electrochem. Soc.*, **151**, A1530 (2004).
[9] J. Christensen, V. Srinivasan, J. Newman, *J. Electrochem. Soc.*, **153**, A560 (2006).
[10] S. Stewart, P. Albertus, V. Srinivasan, I. Plitz, N. Pereira, G. Amatucci, J. Newman, *J. Electrochem. Soc.*, **155**, A253 (2008).
[11] V. R. Subramanian, V. Boovaragavan, V. D. Diwakar, *Electrochem. Solid-State Lt*., **10**, A225 (2007).
[12] V. R. Subramanian, V. Boovaragavan, V. Ramadesigan, M. Arabandi, *J. Electrochem. Soc*., **156**, A260 (2009).
[13] V. R. Subramanian, V. Boovaragavan, V. Ramadesigan, K. Chen, R. D. Braatz, "Model Reformulation and Design of Lithium Ion Batteries," in *Design for Energy and the Environment: Proceedings of the Seventh International Conference on Foundations of Computer-Aided Process Design*, edited by M. M. El-Halwagi and A. A. Linninger, CRC Press, Boca Raton, FL (2009).
[14] R. E. Garcia, Y.-M. Chiang, W. C. Carter, P. Limthongkul, C. M. Bishop, *J. Electrochem. Soc.*, **152**, A255 (2005).
[15] G. Ceder, M. K. Aydinol, A.F. Kohan, *Comput. Mater. Sci.*, **8**, 161 (1997).
[16] N. Akaiwa, K. Thornton, P. W. Voorhees, *J. Comput. Phys.*, **173**, 61 (2001).
[17] S. Kameswaran, L. T. Biegler, *Comp. Chem. Eng.*, **30**, 1560 (2006).
[18] A maximization is written as a minimization by multiplying by –1.
[19] A. Singer, P. Barton, *J. of Global Optimization*, **34**, 159 (2006).
[20] D. Marquardt, *SIAM J. Appl. Math.*, **11**, 431 (1963).
[21] R. D. Braatz, R. C. Alkire, E. G. Seebauer, E. Rusli, R. Gunawan, T. O. Drews, Y. He, *J. of Process Control*, **16**, 193 (2006).
[22] Z. K. Nagy, R. D. Braatz, *J. of Process Control*, **14**, 411 (2004).
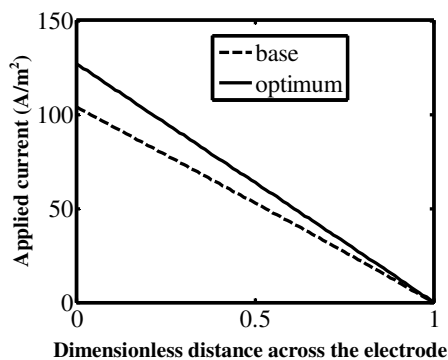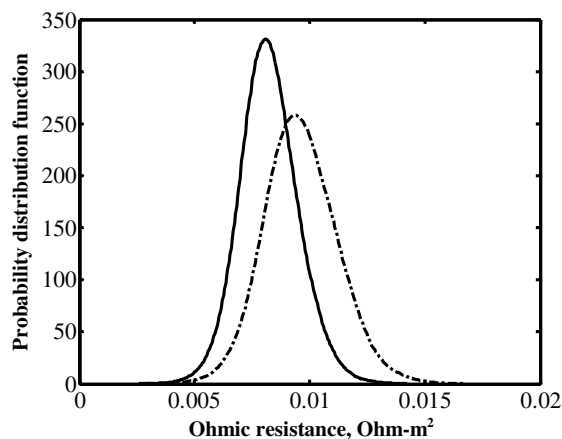
Fig. 6 Applied current profile across the electrode in base-case and optimized designs.
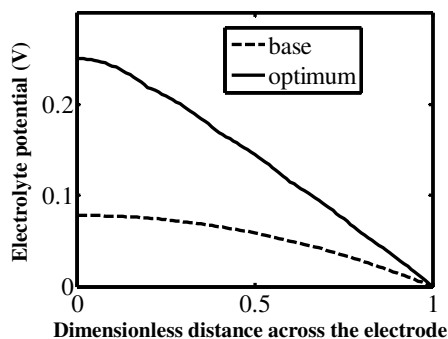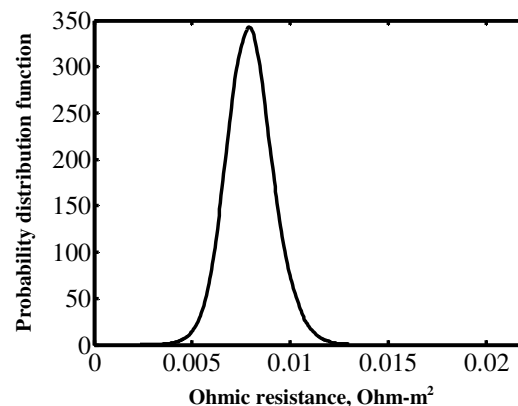

Fig. 7 Electrolyte-phase potential profile in base-case and optimized designs.
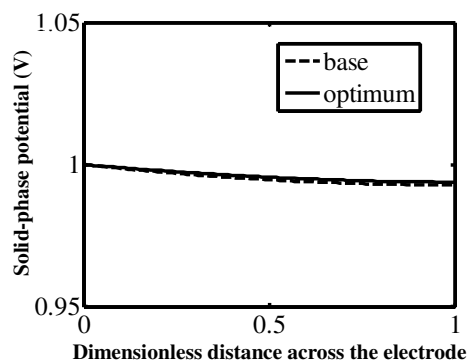
Fig. 8 Solid-phase potential profile in base-case and optimized designs.

Fig. 9 Probability distribution function for the Ohmic resistance for electrodes with spatially-uniform porosities of $\varepsilon = 0.4$ and obtained by optimization ($\varepsilon = 0.21388$).

Fig. 10 Probability distribution function for the Ohmic resistance for the electrode with the optimal spatially-varying porosity profile.